Stability of a telerobotic manipulation system with proximity–based haptic feedback

R. Oboe R. Antonello O. Daud

Dept. of Management and Engineering
University of Padova (Vicenza branch)

E. Grisan

Dept. of Information Engineering
University of Padova

Outline

- **Introduction and motivation**
- **Proposed solution**
  - Bilateral master/slave interface with force feedback
  - 3 DOF optical proximity sensor
- **Control system design**
  - Two–channel force–position bilateral master/slave control architecture
  - Two–level cascaded position & orientation control at slave side
  - Force feedback based on the concept of “virtual constraint”
- **Stability analysis**
  - Stability proof of the slave orientation control by Lyapunov analysis
  - Stability proof of the haptic force feedback based on small gain theorem
- **Experimental results**
- **Conclusions**

Motivation

- Recently, the *Contrast–Enhanced Ultra Sound* (CEUS) examination has been proposed as a promising replacement of *Magnetic Resonance Imaging* for the prognosis of *rheumatoid arthritis* based on visualization of early vascular changes in the *synovium*.

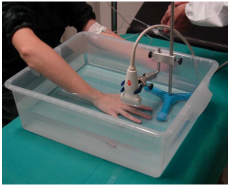

- **Problem**: CEUS image quality depends on the distance and orientation of the ultrasound (US) probe with respect to the surface to be scanned.

  The manual adjustment of the US probe is a demanding task, because the examination is performed in water immersion, where the perceived distance by human eye is affected by water refraction.

Proposed solution

A **bilateral master/slave telerobotic system with haptic feedback** is proposed to

1) automatically adjust the US probe orientation w.r.t. the surface to be scanned
2) provide an haptic–feedback simulating the presence of a "virtual constraint" above the surface to be scanned; this helps the clinician to assess the correct probe distance

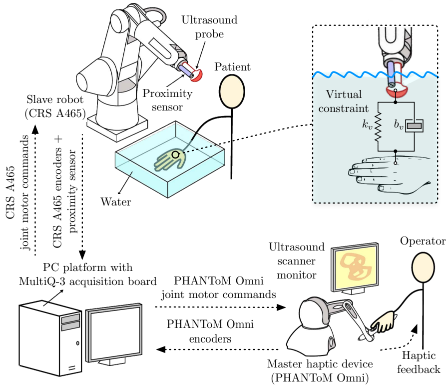

Since CEUS is a *non-contact* exam, a **proximity sensor** is used to accomplish both tasks.

Proposed implementation

Master device

SensAble PHANToM Omni

- 6 DOF positional sensing
- 3 DOF linear force feedback

Slave device

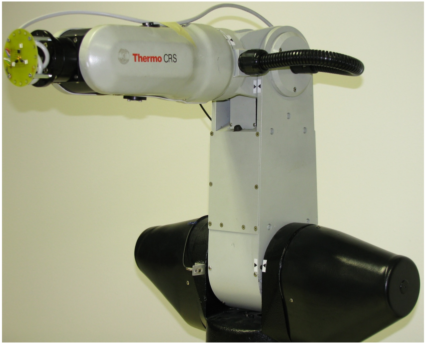

Thermo CRS A465

- 6–axis anthropomorphic manipulator with spherical wrist
- open architecture controller

Proposed implementation

Proximity sensor

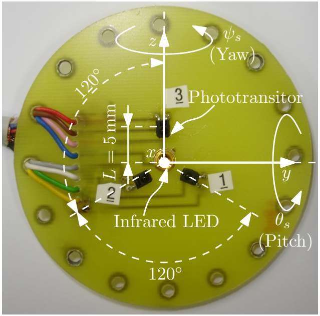

3–DOF optical proximity sensor

- 1 pulsated infrared light source
- 3 phototransitors

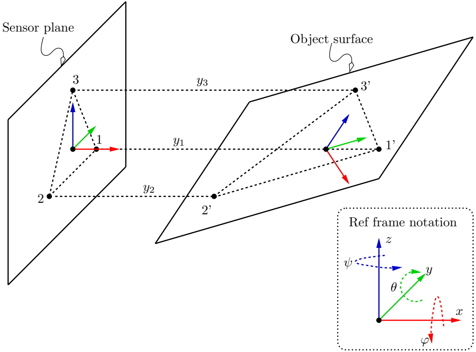

$$d_s \approx \frac{y_1 + y_2 + y_3}{3}$$ Estimated distance

$$\theta_s \approx \operatorname{atan}\left[\frac{2}{3L}\left(y_3 - \frac{y_1 + y_2}{2}\right)\right]$$ Estimated orientation (pitch angle)

$$\psi_s \approx \operatorname{atan}\left(\frac{y_2 - y_1}{\sqrt{3}L}\right)$$ Estimated orientation (yaw angle)

Control system design

- **Control specifications**

a) when no obstacles are detected by the proximity sensor:

- replicate the master movements at the slave side.

b) when an obstacle is detected by the proximity sensor:

- *slave orientation control*: automatically track the normal direction of the surface to be scanned.
- *haptic feedback*: generate a force at the master side to simulate the presence of a "virtual constraint" above the surface to be scanned.

- **Proposed control architecture**: two–channel force–position bilateral master/slave control architecture, with minor modifications of the local position & orientation control at the slave side

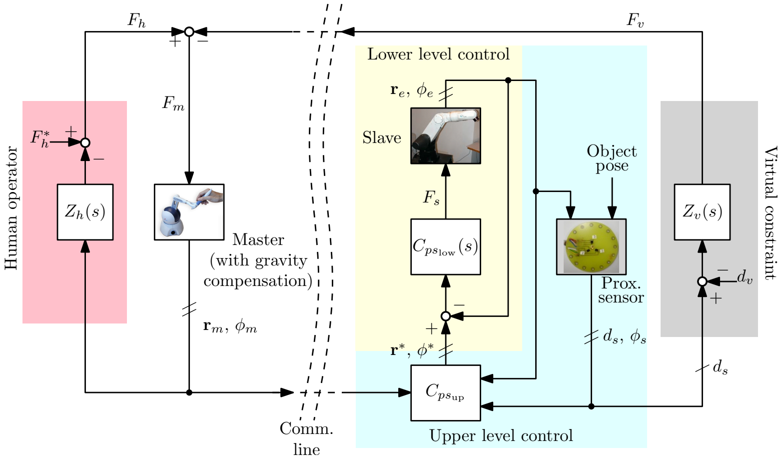

Slave position/orientation controller

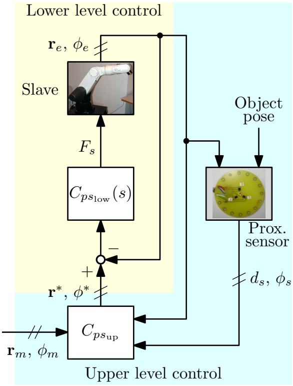

Lower level control

- independent joint control with 6 PD controllers
- reference inputs: end–effector pose, i.e.

$$\boldsymbol{r}^* \triangleq [x^*, y^*, z^*]^T \qquad \begin{pmatrix}\text{end–effector} \\ \text{position ref.}\end{pmatrix}$$

$$\boldsymbol{\phi}^* \triangleq [\varphi^*, \theta^*, \psi^*]^T \qquad \begin{pmatrix}\text{end–effector} \\ \text{orientation ref.}\end{pmatrix}$$

Upper level control

- acts on the reference inputs $\boldsymbol{r}^*$ and $\boldsymbol{\phi}^*$
- when an obstacle is *detected* (object distance below $\approx 35\mathrm{mm}$), aligns the slave end-effector with the object surface, bypassing the master command $\boldsymbol{\phi}_m$

Preliminary notation

1) Rotation matrix specified in terms of the roll, pitch, yaw angles $\boldsymbol{\phi} = [\varphi, \theta, \psi]^T$ relative to the fixed frame

$$\boldsymbol{R}(\boldsymbol{\phi}) = \boldsymbol{R}_z(\psi)\,\boldsymbol{R}_y(\theta)\,\boldsymbol{R}_x(\varphi)$$

$$= \begin{bmatrix} \cos\psi & -\sin\psi & 0 \\ \sin\psi & \cos\psi & 0 \\ 0 & 0 & 1 \end{bmatrix} \begin{bmatrix} \cos\theta & 0 & -\sin\theta \\ 0 & 1 & 0 \\ \sin\theta & 0 & \cos\theta \end{bmatrix} \begin{bmatrix} 1 & 0 & 0 \\ 0 & \cos\varphi & -\sin\varphi \\ 0 & \sin\varphi & \cos\varphi \end{bmatrix}$$

2) Reference frame transformation matrices

$\boldsymbol{R}_r^b(\boldsymbol{\phi})$: reference $\rightarrow$ base

$\boldsymbol{R}_e^b(\boldsymbol{\phi})$: end–effector $\rightarrow$ base

$\boldsymbol{R}_r^e(\boldsymbol{\phi})$: reference $\rightarrow$ end–effector

3) Orientation angles

$\boldsymbol{\phi}_m \triangleq [\varphi_m,\, \theta_m,\, \psi_m]^T$: orientation reference provided by the master

$\boldsymbol{\phi}_e \triangleq [\varphi_e,\, \theta_e,\, \psi_e]^T$: end–effector actual orientation

$\boldsymbol{\phi}_s \triangleq [0,\, \theta_s,\, \psi_s]^T$: surface orientation w.r.t. sensor frame

- **Generation of the orientation reference ϕ^***

  A *finite–state automaton* defines the switching policy between the manual and automatic end–effector orientation control

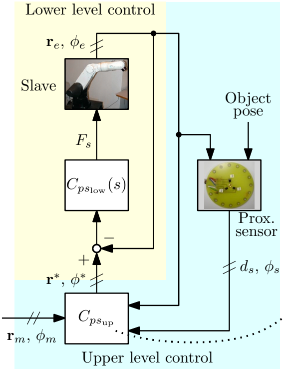

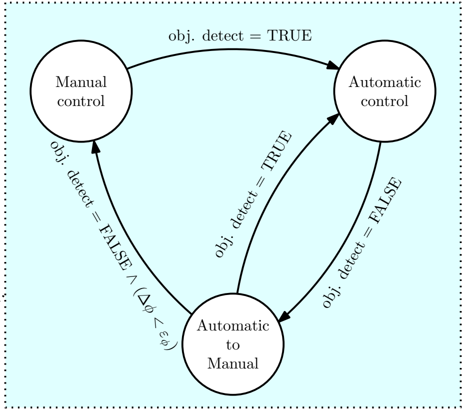

- **Generation of the orientation reference ϕ^***

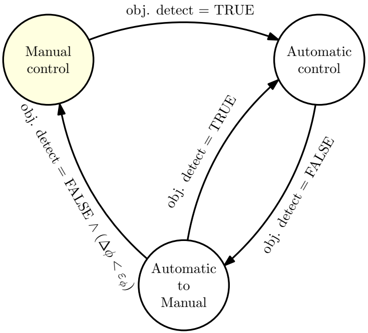

In *manual mode*, the reference ϕ^* is provided by the master (human operator)

$$\phi^* = \phi_m$$

- **Generation of the orientation reference ϕ^***

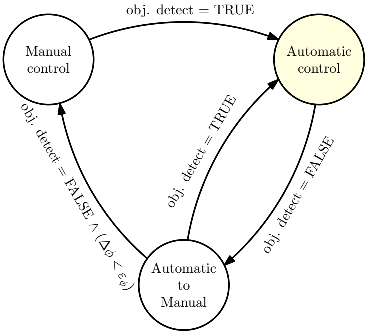

In *automatic mode* (an object is detected by the proximity sensor), the reference ϕ^* is generated with the update law

$$\boldsymbol{R}_r^b\left(\boldsymbol{\phi}^*[k+1]\right) = \boldsymbol{R}_e^b\left(\boldsymbol{\phi}^*[k]\right)\ \boldsymbol{R}_r^e\left(k_\phi\, \boldsymbol{e}_\phi[k]\right)$$

where

$$\boldsymbol{e}_\phi[k] \triangleq \begin{cases} \dfrac{\boldsymbol{\phi}_s[k]}{\|\boldsymbol{\phi}_s[k]\|} & \text{if} \quad \|\boldsymbol{\phi}_s[k]\| \geq \varepsilon_\phi \\ \dfrac{1}{\varepsilon_\phi}\boldsymbol{\phi}_s[k] & \text{if} \quad \|\boldsymbol{\phi}_s[k]\| < \varepsilon_\phi \end{cases}$$

Control system design

- **Generation of the orientation reference ϕ^***

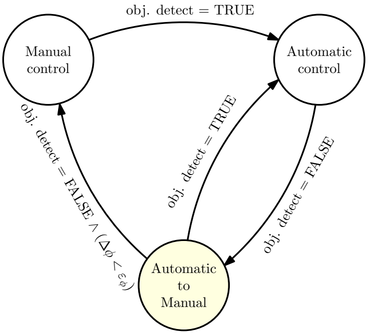

In the *auto–to–manual transition* (the object moves outside the sensor field of view), the reference $\boldsymbol{\phi}^*$ is generated with the update law

$$\boldsymbol{R}_r^b\left(\boldsymbol{\phi}^*[k+1]\right) = \boldsymbol{R}_e^b\left(\boldsymbol{\phi}^*[k]\right)\ \boldsymbol{R}_r^e\left(k_\phi\,\boldsymbol{e}_\phi[k]\right)$$

where

$$\boldsymbol{e}_\phi[k] \triangleq \frac{\Delta\boldsymbol{\phi}[k]}{\|\Delta\boldsymbol{\phi}[k]\|}$$

and $\Delta\boldsymbol{\phi}[k]$ is such that

$$\boldsymbol{R}_r^e\left(\Delta\boldsymbol{\phi}[k]\right) = \boldsymbol{R}_b^e\left(\boldsymbol{\phi}_e[k]\right)\ \boldsymbol{R}_r^b\left(\boldsymbol{\phi}_m[k]\right)$$

- **Generation of the haptic force feedback**

  A force feedback is generated at master side to simulate the presence of a "virtual constraint", atop the surface to be scanned

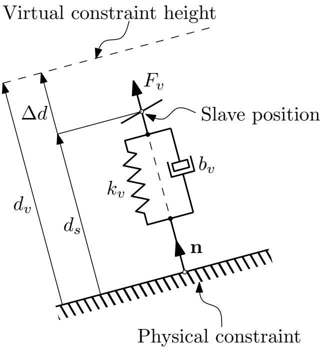

- Force intensity:

$$F_v \triangleq \begin{cases} -b_v \dfrac{d}{dt}\Delta d - k_v \Delta d & \text{if } \Delta d \geq 0 \\ 0 & \text{otherwise} \end{cases}$$

with $\quad \Delta d \triangleq d_v - d_s \quad$ (penetration depth within the "virtual constraint")

- Force direction:

  orthogonal to the physical constraint surface (i.e. parallel to normal vector $\boldsymbol{n}$)

Stability analysis (slave attitude control)

Assumptions

1) the surface to be scanned has a fixed orientation $\boldsymbol{\phi}_d$ in cartesian space, so that

$$\boldsymbol{R}(\boldsymbol{\phi}_d) = \boldsymbol{R}(\boldsymbol{\phi}_e[k])\,\boldsymbol{R}(\boldsymbol{\phi}_s[k]) \quad \forall k \in \mathbb{N}$$

2) the attitude control dynamics is slower than the robot dynamics, so that the lower level control dynamics can be modeled as a unit delay, i.e. $\boldsymbol{\phi}_e[k] = \boldsymbol{\phi}^*[k-1]$

3) the orientation error $\boldsymbol{\phi}_s$ measured by the proximity sensor is small

$$\Downarrow$$

By assumptions 2 and 3, the orientation reference updating law in automatic mode

$$\boldsymbol{R}_r^b\left(\boldsymbol{\phi}^*[k+1]\right) = \boldsymbol{R}_e^b\left(\boldsymbol{\phi}^*[k]\right)\,\boldsymbol{R}_r^e\left(k_\phi\,\boldsymbol{e}_\phi[k]\right) \quad \text{with} \quad \boldsymbol{e}_\phi[k] \triangleq \begin{cases} \dfrac{\boldsymbol{\phi}_s[k]}{\|\boldsymbol{\phi}_s[k]\|} & \text{if} \quad \|\boldsymbol{\phi}_s[k]\| \geq \varepsilon_\phi \\ \dfrac{1}{\varepsilon_\phi}\boldsymbol{\phi}_s[k] & \text{if} \quad \|\boldsymbol{\phi}_s[k]\| < \varepsilon_\phi \end{cases}$$

becomes

$$\boldsymbol{R}(\boldsymbol{\phi}_e[k+2]) = \boldsymbol{R}(\boldsymbol{\phi}_e[k+1])\,\boldsymbol{R}(\kappa\,\boldsymbol{\phi}_s[k]) \quad \text{with} \quad \kappa \triangleq k_\phi/\varepsilon_\phi$$

[. . .]

Stability analysis (slave attitude control)

Assumptions

1) the surface to be scanned has a fixed orientation $\boldsymbol{\phi}_d$ in cartesian space, so that

$$\boldsymbol{R}(\boldsymbol{\phi}_d) = \boldsymbol{R}(\boldsymbol{\phi}_e[k])\,\boldsymbol{R}(\boldsymbol{\phi}_s[k]) \quad \forall k \in \mathbb{N}$$

2) the attitude control dynamics is slower than the robot dynamics, so that the lower level control dynamics can be modeled as a unit delay, i.e. $\boldsymbol{\phi}_e[k] = \boldsymbol{\phi}^*[k-1]$

3) the orientation error $\boldsymbol{\phi}_s$ measured by the proximity sensor is small

$$\Downarrow$$

[...] From assumption 1 it follows that

$$\boldsymbol{R}(\boldsymbol{\phi}_s[k]) = \boldsymbol{R}(\boldsymbol{\phi}_e[k])^T\,\boldsymbol{R}(\boldsymbol{\phi}_d) \tag{1}$$

After post–multiplying the transpose of both sides of the orientation reference updating law

$$\boldsymbol{R}(\boldsymbol{\phi}_e[k+2]) = \boldsymbol{R}(\boldsymbol{\phi}_e[k+1])\,\boldsymbol{R}(\kappa\,\boldsymbol{\phi}_s[k]) \quad \text{with} \quad \kappa \triangleq k_\phi/\varepsilon_\phi$$

obtained before by $\boldsymbol{R}(\boldsymbol{\phi}_d)$ and using (1), the following equation results

$$\boldsymbol{R}(\boldsymbol{\phi}_s[k+2]) = \boldsymbol{R}(\kappa\,\boldsymbol{\phi}_s[k])^T\,\boldsymbol{R}(\boldsymbol{\phi}_s[k+1])$$

Stability analysis (slave attitude control)

[. . .] For small Euler angles $\delta\boldsymbol{\phi} \triangleq [\delta\varphi, \delta\theta, \delta\psi]^T$, the generic rotation matrix $\boldsymbol{R}(\delta\phi)$ can be approximated by its linearized version

$$\boldsymbol{R}(\delta\boldsymbol{\phi}) \approx \begin{bmatrix} 1 & -\delta\varphi & \delta\theta \\ \delta\varphi & 1 & -\delta\psi \\ -\delta\theta & \delta\psi & 1 \end{bmatrix} \tag{2}$$

By using the small angle approximation (2) for each rotation matrix in the equation

$$\boldsymbol{R}\left(\boldsymbol{\phi}_s[k+2]\right) = \boldsymbol{R}\left(\kappa\,\boldsymbol{\phi}_s[k]\right)^T \boldsymbol{R}\left(\boldsymbol{\phi}_s[k+1]\right)$$

obtained before, and neglecting high order terms, the following set of independent equations for the angles $\delta\varphi_s$, $\delta\theta_s$ and $\delta\psi_s$ is obtained

$$\begin{aligned} \delta\varphi_s[k] &= 0 \\ \delta\theta_s[k+2] &= -\kappa\,\delta\theta_s[k] + \delta\theta_s[k+1] \\ \delta\psi_s[k+2] &= -\kappa\,\delta\psi_s[k] + \delta\psi_s[k+1] \end{aligned}$$

Then, the linearized (decoupled) dynamics of θ_s and ψ_s is *asymptotically stable* (and hence the slave end–effector orientation $\boldsymbol{\phi}_e$ converges locally to $\boldsymbol{\phi}_d$) iff the roots of the polynomial $p(z) \triangleq z^2 - z + \kappa$ lie within the unit circle $|z| = 1$.

Stability analysis (haptic force feedback)

Assumptions

1) end–effector movements are small and directed orthogonally to the surface to be scanned
2) communication time delay between master and slave is negligible
3) mechanical impedances are approximated with LTI models

(Master impedance)	(Slave impedance)	(Human impedance)	(Virtual constr. impedance)
$Z_m(s) \approx M_m s^2 + b_m s$	$Z_s(s) \approx M_s s^2 + b_s s$	$Z_h(s) \approx M_h s^2 + b_h s + k_h$	$Z_v(s) \approx b_v s + k_v$

$$\Downarrow$$

The force feedback loop reduces to the interconnection of two LTI systems Σ_1 and Σ_2

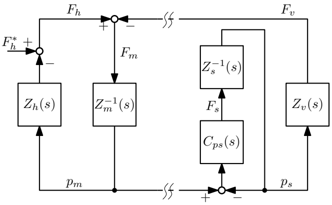

$\longrightarrow$

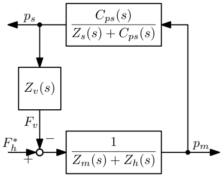

$\longrightarrow$ [. . .]

Stability analysis (haptic force feedback)

$[\ldots] \quad \longrightarrow$

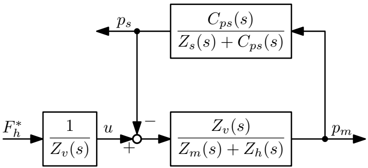

$$\Sigma_1 : G_1(s) \triangleq \frac{C_{ps}(s)}{Z_s(s)+C_{ps}(s)}$$

$$\Sigma_2 : G_2(s) \triangleq \frac{Z_v(s)}{Z_m(s)+Z_h(s)}$$

As usually done in standard practice, the low level controller $C_{ps}(s)$ is a PD controller tuned to cancel the slave impedance zero at $s = -b_s/M_s$, i.e.

$$C_{ps}(s) = k_p + k_d\, s \qquad \text{with} \qquad k_d/k_p = M_s/b_s$$

$$\Downarrow$$

$$G_1(s) = \frac{1}{(b_s/k_p)s+1}\,, \qquad G_2(s) = \frac{b_v s + k_v}{(M_m+M_h)s^2+(b_m+b_h)s+k_h}$$

Stability analysis (haptic force feedback)

- Since all the poles of $G_{1,2}(s)$ lie in the open left–half plane, then both $\Sigma_{1,2}$ are finite–gain $\mathcal{L}_p$ stable for each $p \in [1, +\infty]$. (1)

  Say $\gamma_{1,2}$ the $\mathcal{L}_p$ gains of $\Sigma_{1,2}$: then, a sufficient condition for the feedback connection of $\Sigma_{1,2}$ with input u and outputs $p_{m,s}$ to be finite–gain $\mathcal{L}_p$ stable is that $\gamma_1 \, \gamma_2 < 1$ (*small–gain theorem*). (2)

- The $\mathcal{L}_2$ gains can be easily computed as (3)

$$\gamma_{1,2} = \|G_{1,2}\|_\infty = \sup_{\omega \in \mathbb{R}} |G_{1,2}(j\omega)|$$

  Since

$$\gamma_1 = \left\| \frac{1}{(b_s/k_p)s + 1} \right\|_\infty = 1$$

  then the feedback loop (with input u) is $\mathcal{L}_2$ stable when the parameters b_v and k_v of the virtual impedance $Z_v(s)$ are chosen so that $\gamma_2 < 1$.

$(1, 2, 3)$ see Corollary 5.2 and Theorems 5.4, 5.6 in H.K.Khalil, *Nonlinear Systems*, 3rd ed. Prentice Hall, 2002

Stability analysis (haptic force feedback)

$$\gamma_2 < 1 \quad \Leftrightarrow \quad |k_v + b_v\, j\omega| < \left|k_h - (M_m + M_h)\,\omega^2 + (b_m + b_h)\, j\omega\right| \quad \forall\, \omega \in \mathbb{R}$$

$$\Updownarrow$$

$$(M_m + M_h)^2\omega^4 + \left[(b_m + b_h)^2 - b_v^2 - 2\,k_h(M_m + M_h)\right]\omega^2 + (k_h^2 - k_v^2) > 0$$

$$\Updownarrow$$

<u>Condition for b_v and k_v</u>

$$\left[(b_m + b_h)^2 - b_v^2 - 2\,k_h(M_m + M_h)\right]^2 - 4\,(M_m + M_h)^2(k_h^2 - k_v^2) < 0$$

- Finally, the feedback loop with input F_h^* is also finite–gain $\mathcal{L}_2$ stable, since the system with transfer function $1/Z_v(s)$ is finite–gain $\mathcal{L}_2$ stable.
- *Note*: thanks to the small gain theorem, the stability result is still valid even in the case of non–negligible communication time delay.

Stability analysis (haptic force feedback)

Condition for b_v and k_v

$$\left[(b_m + b_h)^2 - b_v^2 - 2\,k_h(M_m + M_h)\right]^2 - 4\,(M_m + M_h)^2(k_h^2 - k_v^2) < 0$$

$$\Updownarrow \quad M \triangleq M_m + M_h\,,\ b \triangleq b_m + b_h$$

Admissible region in (b_v^2, k_v^2)–plane

$$k_v^2 < -\frac{1}{4M^2}b_v^4 + \frac{\alpha}{2M^2}b_v^2 + \left(k_h^2 - \frac{\alpha^2}{4M^2}\right) \quad \text{with} \quad \alpha \triangleq b^2 - 2Mk_h$$

The admissible region

- is not empty for any choice of the positive parameters M, b, k_h, since the concave parabola at the RHS has a positive intersection with the b_v^2–axis at $b_v^2 = b_h^2$.
- depends on the parameters M_h, b_h, k_h of the human arm impedance $Z_h(s)$

$$\Downarrow$$

an identification experiment is required.

Identification experiment

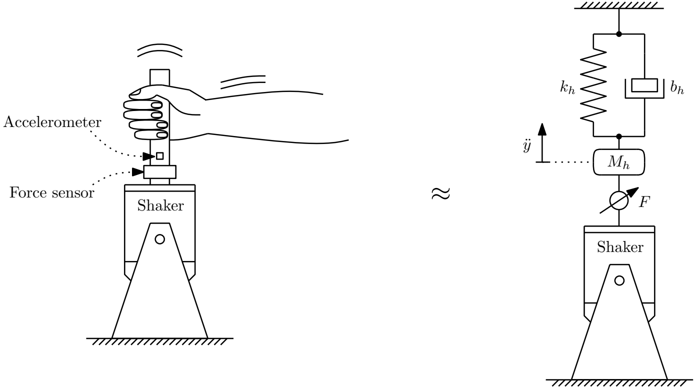

Given the acceleration and force measurement recorded during a band–limited random shaking motion, the parameters M_h, b_h, k_h of the human impedance $Z_h(s)$ are estimated using conventional parametric identification methods.

"Soft grasp" test

Experimental test

Identification results

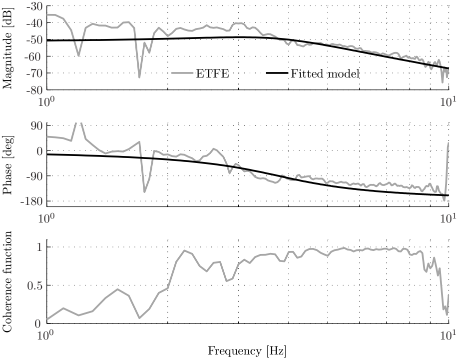

M_h [kg]	b_h [Ns/m]	k_h [N/m]
0.707	7.78	247.22

"Hard grasp" test

Experimental test

Identification results

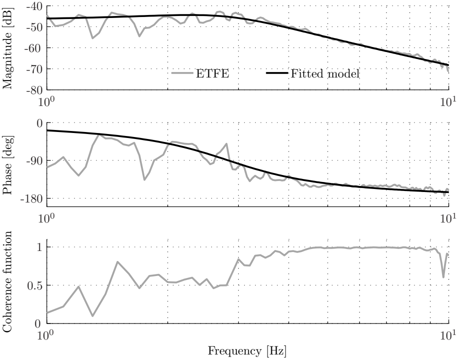

M_h [kg]	b_h [Ns/m]	k_h [N/m]
0.884	6.39	409.35

Identification of human arm impedance

"Soft grasp" test

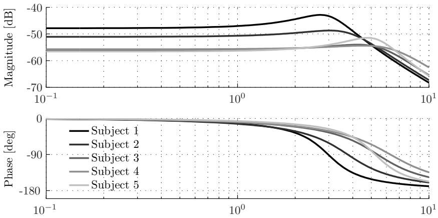

	M_h [kg]	b_h [Ns/m]	k_h [N/m]
Subject 1	0.707	7.78	247.22
Subject 2	0.641	12.73	358.49
Subject 3	0.558	16.48	640.07
Subject 4	0.393	15.27	612.48
Subject 5	0.622	11.87	674.36
Max:	0.707	16.48	674.36
Min:	0.393	7.78	247.22
Mean:	0.584	12.82	506.52

"Hard grasp" test

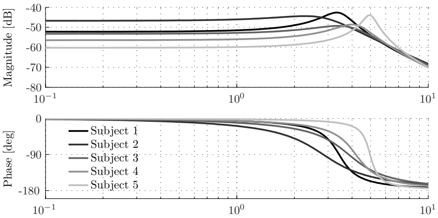

	M_h [kg]	b_h [Ns/m]	k_h [N/m]
Subject 1	0.884	6.39	409.35
Subject 2	0.689	10.31	217.55
Subject 3	0.790	12.83	460.39
Subject 4	0.961	10.50	664.77
Subject 5	1.053	5.04	1027.31
Max:	1.053	12.83	1027.31
Min:	0.689	5.04	217.55
Mean:	0.876	9.01	555.87

Stability analysis (haptic force feedback)

Admissible region boundary

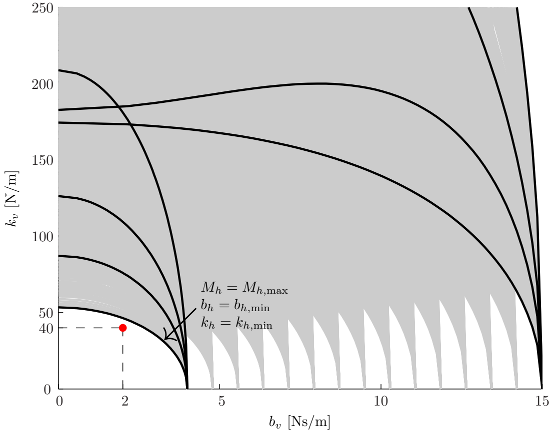

Parameters space

	Min	Max
M_h [kg]	0.4	1.1
b_h [Ns/m]	4	15
k_h [N/m]	200	1100

Notes:

1) gray lines refer to $15 \times 15 \times 15$ triplets of parameters uniformly distributed over the parameters space.
2) black lines refer to the "corners" of the parameters space.

The experimental choice $(b_v, k_v) = (2, 40)$ guarantees a stable operation for any choice of the human arm impedance parameters (within the specified ranges).

Automatic alignment test

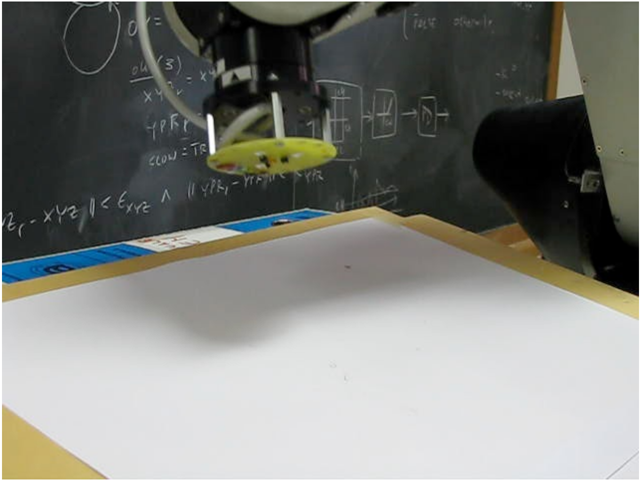

Experimental tests

Surface scansion test

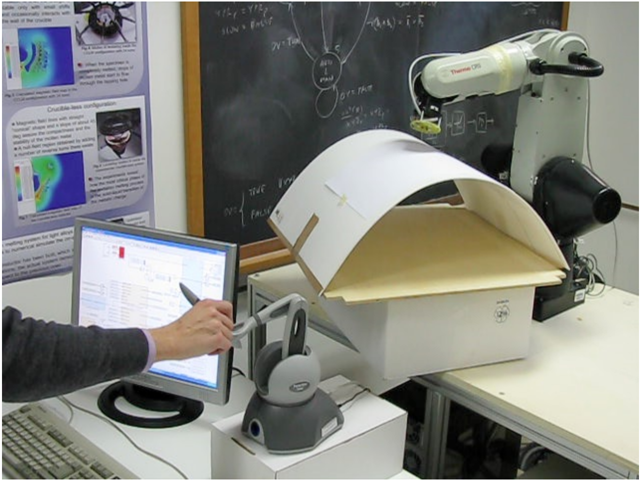

Experimental results

Alignment process

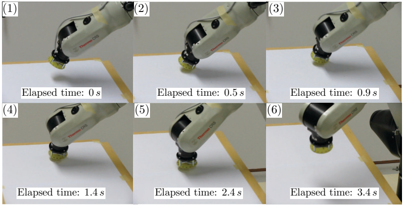

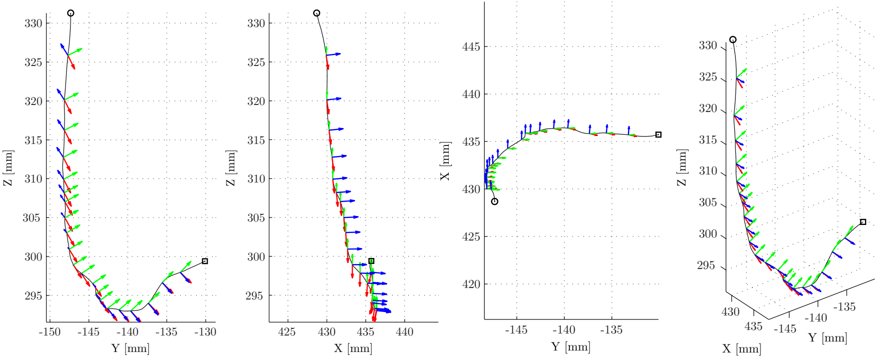

Experimental results

Position

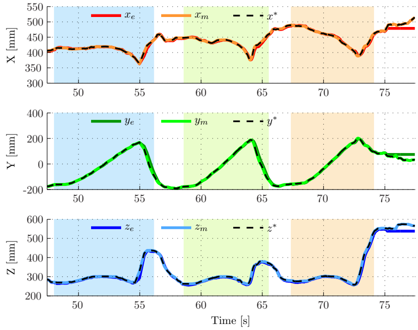

Orientation

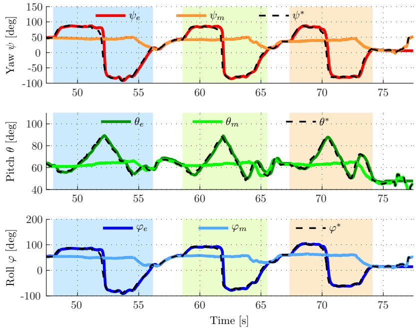

Haptic force feedback

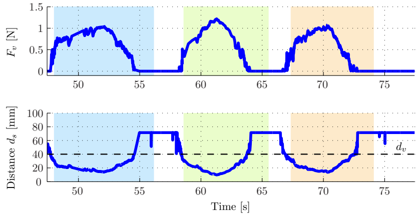

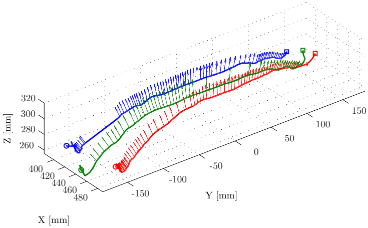

Conclusions

- Proposed a master/slave system with haptic feedback to aid the clinician to correctly handle the US probe during a CEUS examination.
- Experimental results have shown the capability of the proposed architecture to maintain the correct orientation and safeguard distance of the robot end–effector w.r.t. the surface to be scanned.
- A haptic feedback has been properly generated to simulate the presence of a "virtual constraint" above the surface to be scanned, which helps the clinician to adjust the US probe distance in order to get an enhanced image quality.
- Future research activities will be devoted to the
  - development of a new proximity sensor, more suitable for surfaces with high curvatures (e.g. around finger joints) and less sensitive to variations of surface reflectivity.
  - integration of the US probe and additional safety and protection systems in the existing setup.